Hydrogen Transfer from $[MeB(C_6F_5)_3]^-$ to the Methyl Group of L_2MMe^+ (M = Ti, Zr) as a Deactivation Pathway in Olefin Polymerization Catalysis: A Combined Quantum Mechanics and Molecular Mechanics Investigation

Tebikie Wondimagegn, Kumar Vanka, Zhitao Xu, and Tom Ziegler*

Department of Chemistry, University of Calgary, Calgary, Alberta, Canada T2N 1N4

Received October 11, 2003

A combined quantum-mechanical (QM) and molecular-mechanical (MM) model (QM/MM) has been used to investigate hydrogen transfer from the methyl group in $[MeB(C_6F_5)_3]^-$ to the growing chain of a number of cationic single-site olefin polymerization catalysts. This reaction, which produces methane or higher alkanes, is a possible deactivation pathway in metal-catalyzed olefin polymerization. The cationic catalyst systems include $(NPR_3)_2TiR^+$, $(Cp)(NPR_3)TiR^+$, $(Cp)(NCR_2)TiR^+$, $(Cp)(SiMe_2NR)TiR^+$, and $(Cp)(OSiR_3)TiR^+$. For comparison, the corresponding zirconium catalyst systems have also been considered. We find hydrogen transfer to be more facile for titanium catalysts than for the corresponding zirconium systems. Furthermore, steric bulk and electron-donating ligands help to suppress hydrogen transfer. With $R = CH_3$, decomposition by hydride transfer is likely to take place for all the titanium catalysts at about 100 °C. However, for longer chains the decomposition temperature increases to 250 °C.

Introduction

Bis(cyclopentadienyl) (bis-Cp) complexes of the early transition metals are highly effective homogeneous olefin polymerization catalysts, but extensive patent coverage has spurred the development of new catalysts that do not exclusively contain the bis-Cp ligand framework.[1] Numerous efforts have been made to explore the potential of other ligand and catalyst systems. The most common way of developing such catalyst systems has been to replace one or both of the Cp ligands in the metallocenes by other donor groups. A notable example of this approach is the so-callled "constrained-geometry catalysts" first introduced by Bercaw[2] and later developed by Dow[3] and Exxon,[4] based on the Cp−amido ligand. Nowadays, a wide range of $Cp(L)TiX_2$ catalysts (L = OR,[5] NCR_2,[6] NPR_3,[7] NR_2,[8] SR,[9] and alkyl[10]) have been prepared and tested in catalytic olefin polymerization. When activated by cocatalysts such as methylaluminoxane (MAO), $B(C_6F_5)_3$, and $[A]^+[B(C_6F_5)_4]^-$ ($A = CPh_3$, HNR_3), the complexes have been found to provide catalysts with moderate to high activity, making them viable alternatives to the bis(cyclopentadienyl) systems.

However, the new catalyst systems have also been found to exhibit a greater tendency toward deactivating side reactions, leading to the eventual poisoning of the catalysts and thereby decreasing their productivity. An understanding of the deactivation mechanisms along with modifications that could prevent their occurrence would aid greatly in improving the design and development of nonmetallocene catalyst systems.

Some experimental work[6,11] with $B(C_6F_5)_3$ as the cocatalyst has been conducted to elucidate the possible reaction mechanisms. The principal processes of deactivation, as shown in Scheme 1, are C−H activation,

* To whom correspondence should be addressed. E-mail: ziegler@ucalgary.ca.

(1) (a) Britovsek, G. P.; Gibson, V. C.; Waas, D. F. *Angew. Chem., Int. Ed.* **1999**, *38*, 429. (b) Liang, L.-C.; Schrock, R. R.; Davis, W. M.; McConville, D. H. *J. Am. Chem. Soc.* **1999**, *121*, 5797. (c) Baumann, R.; Stumpf, R.; Davis, W. M.; Liang, l.-C.; Schrock, R. R. *J. Am. Chem. Soc.* **1999**, *121*, 7822. (d) Zhang, S.; Piers, W. E.; Gao, X.; Parvez, M. *J. Am. Chem. Soc.* **2000**, *122*, 5499. (e) Guerin, F.; Stewart, J. C.; Beddie, C.; Stephan, D. W. *Organometallics* **2000**, *19*, 2994. (f) Yue, N.; Hollink, E.; Guerin, F.; Stephan, D. W. *Organometallics* **2001**, *20*, 4424.

(2) (a) Piers, W. E.; Shapiro, P. J.; Bunel, E. E.; Bercaw, J. E. *Synlett* **1990**, *1*, 74. (b) Shapiro, P. J.; Cotter, W. D.; Schaefer, W. P.; Labinger, J. A.; Bercaw, J. E. *J. Am. Chem. Soc.* **1994**, *116*, 4623.

(3) Stevens, J. C.; Timmers, F. J.; Wilson, D. R.; Schmidt, G. F.; Nickias, P. N.; Rosen, R. K.; Knight, G. W.; Lai, S. Eur. Pat. Appl. EP 416 815-A2, 1991 (Dow Chemical Corp.).

(4) Canich, J. M.; Hlatky, G. G.; Turner, H. W. PCT Appl. WO-A-00333, 1992 (Exxon Chemical Co.).

(5) (a) Vilardo, J. S.; Thorn, M. G.; Fanwick, P. E.; Rothwell, I. P. *Chem. Commun.* **1998**, 2425. (b) Thorn, M. G.; Vilardo, J. S.; Fanwick, P. E.; Rothwell, I. P. *Chem. Commun.* **1998**, 2427. (c) Sarsfield, M. J.; Ewart, S. W.; Tremblay, T. L.; Roszak, A. W.; Baird, M. C. *J. Chem. Soc., Dalton Trans.* **1997**, 3097. (d) Ewart, S. W.; Sarsfield, M. J.; Jeremic, D.; Tremblay, T. L.; Williams, E. F.; Baird, M. C. *Organometallics* **1998**, *17*, 1502.

(6) Zhang, S.; Piers, W. E.; Gao, X.; Parvez, M. *J. Am. Chem. Soc.* **2000**, *122*, 5499.

(7) Stephan, D. W.; Stewart, J. C.; Guerin, F.; Spence, R. E. v. H.; Xu, W.; Harrison, D. G. *Organometallics* **1999**, *18*, 1116.

(8) . (a) Bai, Y.; Roesky, H. W.; Noltmeyer, M. *Z. Anorg. Allg. Chem.* **1991**, *31*, 3887. (b) Schiffino, R. S.; Crowther, D. J. U.S. Patent No. 5,625,016, 1997 (Exxon Chemical Co.).

(9) Klapötke, T.; Laskowski, R.; Köpf, H. *Z. Naturforsch., B* **1987**, *42*, 777.

(10) (a) Ewart, S. W.; Baird, M. C. *Top. Catal.* **1999**, *7*, 1. (b) Mena, M.; Royo, P.; Serrano, R.; Pellinghelli, A.; Tiripicchio, A. *Organometallics* **1989**, *8*, 476.

(11) (a) Kickham, J. E.; Guerin, F.; Stephan, D. W. *J. Am. Chem. Soc.* **2002**, *124*, 11486. (b) Guerin, F.; Stephan, D. W. *Angew. Chem., Int. Ed.* **2000**, *39*, 1298.

10.1021/om034232t CCC: $27.50
Publication on Web 04/29/2004

Scheme 1. The Different Deactivation Pathways Observed Experimentally

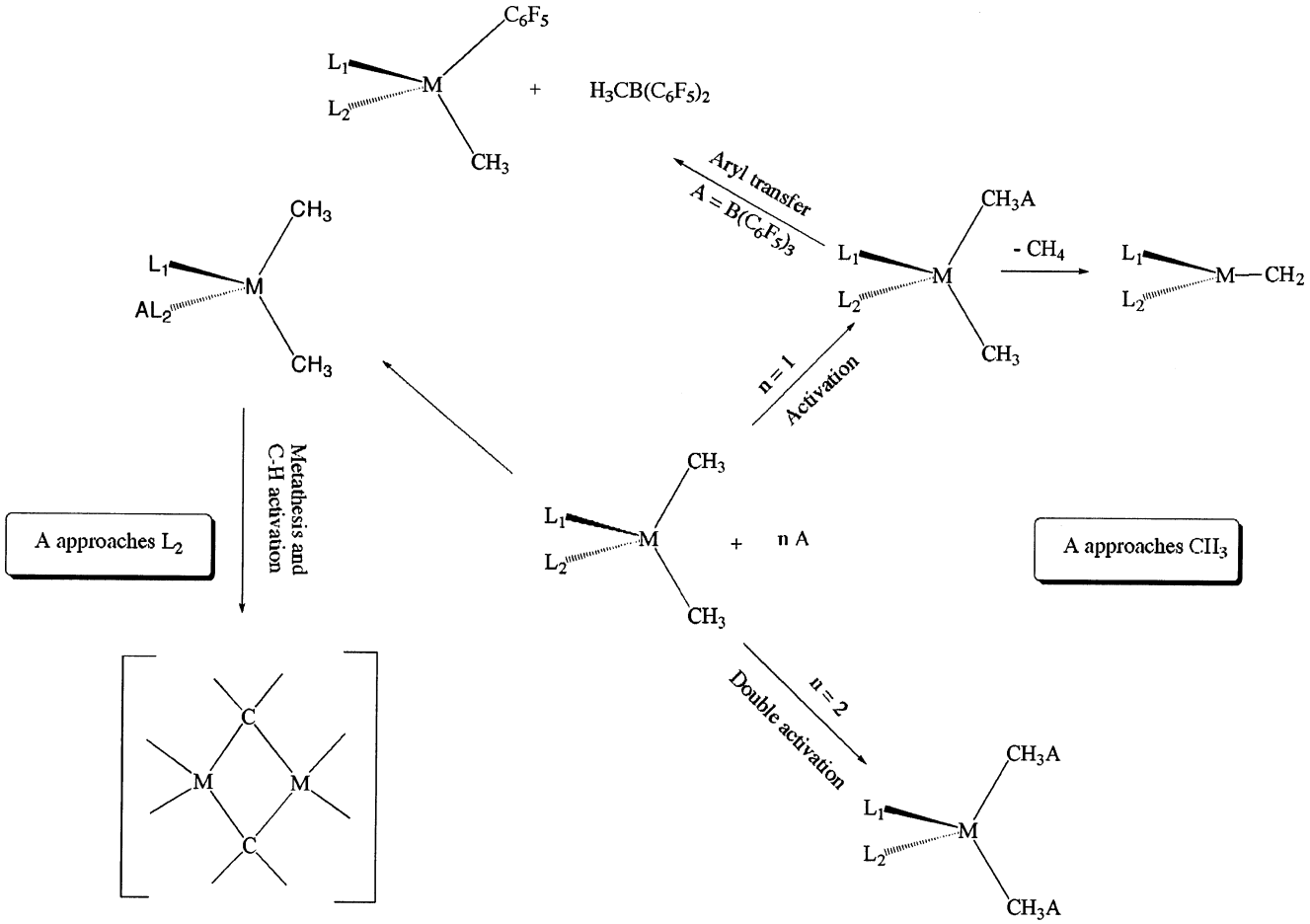

metathesis, aryl transfer from the counterion to the metal, and double activation of the precatalyst by the cocatalyst.

The experimentally observed deactivation pathways prompted us to undertake a theoretical study of hydrogen transfer from the counterion $[MeB(C_6F_5)_3]^-$ to the methyl chain of the cation L_2MMe^+, as shown in Scheme 1. To our knowledge, this is the first theoretical investigation of hydrogen transfer from the counterion to the methyl chain for the catalyst systems depicted in Figure 1. The process has been studied experimentally by Piers et al. for the $(Cp)(NCR_2)TiMe^+$ system.[6]

Computational Details and Methods

Density functional theory calculations were carried out using the Amsterdam Density Functional (ADF) program system, developed by Baerends et al.[12] and vectorized by Ravenek.[13] The numerical integration scheme applied was developed by te Velde et al.,[14] and the geometry optimization procedure was based on the method of Verslius and Ziegler.[15]

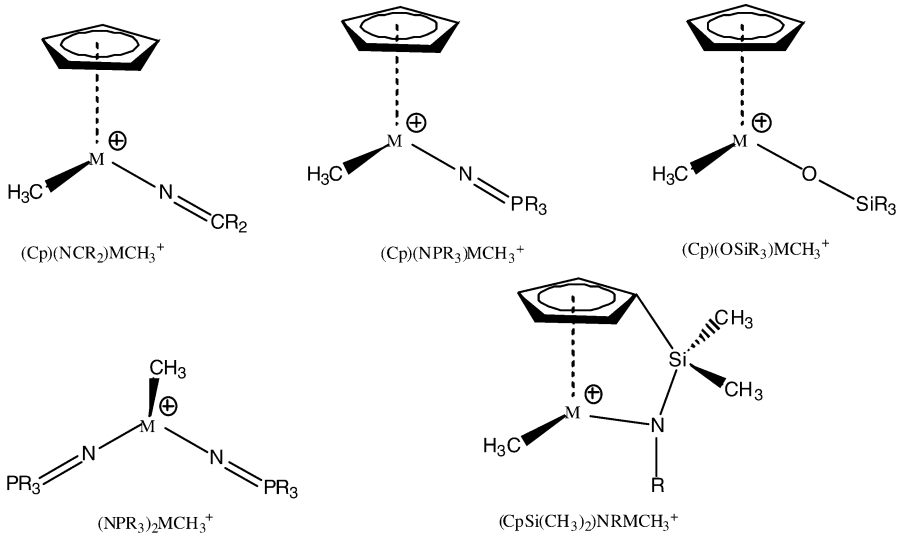

Figure 1. Structures of the catalyst systems under investigation.

Table 1. Activation Energies (kcal/mol) for Hydrogen Transfer in Titanium Systems[a]

	R	
cat.	H	^{t}Bu
$(Cp)(NCR_2)TiMe^+$	18.9 (21.0)[b]	21.9 (22.4)
$(Cp)(NPR_3)TiMe^+$	18.7 (20.4)	23.3 (27.6)
$(NPR_3)_2TiMe^+$	19.1 (22.4)	24.3 (28.9)
$(Cp)(OSiR_3)TiMe^+$	19.2 (19.7)	21.9 (24.9)
$(CpSiMe_2NR)TiMe^+$	19.4 (22.2)	21.5 (24.2)

[a] The counterion is $B(C_6F_5)_3Me^-$ in all cases. [b] In solution. Solvent: cyclohexane ($\epsilon = 2.023$).

Table 2. Activation Energies (kcal/mol) for Hydrogen Transfer in Zirconium Systems[a]

	R	
cat.	H	^{t}Bu
$(Cp)(NCR_2)ZrMe^+$	*b*	24.2
$(Cp)(NPR_3)ZrMe^+$	22.6	26.5
$(NPR_3)_2ZrMe^+$	*b*	27.3
$(Cp)(OSiR_3)ZrMe^+$	23.7	24.7
$(CpSiMe_2NR)ZrMe^+$	*b*	27.3
$(1,2\text{-}Me_2Cp)_2ZrMe^+$	26.0	

[a] The counterion is $B(C_6F_5)_3Me^-$ in all cases. [b] We were unable to locate the transition state, due to a competition between hydrogen and aryl transfer.

Slater-type double-ς plus polarization basis sets were employed for H, B, C, N, O, F, Si, P, and Cl atoms, while triple-ς plus polarization basis sets were used for Ti and Zr atoms. All the calculations used the PW91 exchange-correlation functional.[16]

Combined quantum-mechanical (QM) and molecular-mechanical (MM) models (QM/MM) have been applied throughout this study. In this model, the perfluorophenyl groups (C_6F_5) in the counterion, $[MeB(C_6F_5)]^-$, were replaced by MM atoms and Cl atoms were used to cap the QM system. The MM atoms were described using the SYBYL/TRIPOS 5.2 force field constants.[17] The code for QM/MM in ADF has been implemented by Woo et al.[18] The QM/MM model for $[MeB(C_6F_5)_3]^-$ has been validated in a previous study.[19] The solvation energies based on gas-phase geometries were calculated by the conductor-like screening model (COSMO)[20] with a dielectric constant of 2.023 to represent cyclohexane as the solvent. The radii used for the atoms (in Å) were as follows: C, 2.0; H, 1.16; B, 1.15; N, 1.5; O, 1.5; F, 1.2; Zr, 2.4; Ti, 2.3; P, 1.7; Cl, 2.1; Si, 2.2; Al, 2.3.

Results and Discussion

The present investigation aims to address the following questions using combined quantum-mechanical and molecular-mechanical calculations. (1) How important are the electronic and steric effects of the ancillary ligands in modulating hydrogen transfer barriers? (2) How do the entropy of activation and concentration of the monomer affect the crossover temperature T_x, at which the rate of deactivation by hydrogen transfer becomes equal to the rate of olefin polymerization by monomer insertion? The answers to the above questions are important for devising ways in which the deactivation could be reduced or eliminated entirely.

Activation Energies for Hydrogen Transfer. Tables 1 and 2 present hydrogen transfer barriers for the different catalyst systems studied in this work. As seen from Table 1, the hydrogen transfer barriers for the generic systems in which alkyl groups on the ancillary ligands are replaced by hydrogens fall in the narrow range 18.7−19.4 kcal/mol. In all cases, the zirconium complexes have a higher barrier than the corresponding titanium systems. This indicates that the M−C bond is stronger for M = Zr than M = Ti. As shown in Table 2, we are unable to locate a transition state for $(Cp)(NCH_2)ZrMe^+$, $(NPH_3)_2ZrMe^+$, and the constrained-geometry catalyst systems. This is due to a competition between hydrogen and aryl transfer. Ongoing work in our laboratory, focusing on aryl (C_6F_5) transfer from the counterion $[MeB(C_6F_5)]^-$ to the cationic metal center, will be reported in a separate paper on this topic.

Replacing the hydrogen atoms, as shown in Tables 1 and 2, with *tert*-butyl groups increases the barrier, suggesting that steric factors play a major role in modulating the transfer barrier. Although ligands with different electronic properties do not significantly change the activation barrier for the generic systems, these effects are pronounced when *tert*-butyl substituents are employed. An example of this is the hydrogen transfer barrier difference between $(Cp)(OSiR_3)TiMe^+$ (21.9 kcal/mol) and $(Cp)(NPR_3)TiMe^+$ (23.3 kcal/mol) complexes. These complexes are isosteric, and we believe that the observed difference in the activation barrier is due to the different donor abilities of the siloxy and phosphinimide ligands. Therefore, for systems with similar steric properties, electron-donating substituents favor a higher activation barrier. The lower barriers computed for ketimide and the constrained-geometry catalyst are mainly due to steric effects. The steric bulk of bis(phosphinimide) and phosphinimide ligands is considerably larger than that of ketimide and the constrained-geometry catalysts. Presumably, this is reflected by the higher barriers reported for the bis(phosphinimide) and phosphinimide catalysts.

Piers et al.[6] have examined the mechanisms of methane elimination for the ketimide catalyst systems with $B(C_6F_5)_3$ as an initiator. This is basically a hydrogen transfer reaction from the bridging methyl group to the growing chain. Kinetic studies on the decomposition of this ligand show the reaction to be first order with respect to the concentration of the catalyst. They reported activation parameters of $\Delta H^{\ddagger}_d = 20.6$ kcal/mol and $\Delta S^{\ddagger}_d = -8.5$ cal/(mol K). The barrier of 21.9 kcal/mol calculated for this system is in good agreement with the values reported above (see Table 1). Piers et al. measured a substantial kinetic isotopic effect ($k_H/k_D = 9.1$), consistent with the partial C−H bond breaking in the transition state found in our calculation (see Table

(12) (a) Baerends, E. J.; Ellis, D. E.; Ros, P. *Chem. Phys.* **1973**, *2*, 41. (b) Baerends, E. J.; Ros, P. *Chem. Phys.* **1973**, *2*, 52. (c) te Velde, G.; Baerends, E. J. *J. Comput. Phys.* **1992**, *92*, 84. (d) Fonseca, C. G.; Visser, O.; Snijders, J. G.; te Velde, G.; Baerends, E. J. In *Methods and Techniques in Computational Chemistry, METECC-95*; Clementi, E., Corongiu, G., Eds.; STEF; Cagliari, Italy, 1995; p 305.
(13) Ravenek, W. In *Algorithms and Applications on Vector and Parallel Computers*; te Riele, H. J. J., Dekker, T. J., van de Horst, H. A., Eds.; Elsevier: Amsterdam, 1987.
(14) (a) te Velde, G.; Baerends, E. J. *J. Comput. Chem.* **1992**, *99*, 84. (b) Boerrigter, P. M.; te Velde, G.; Baerends, E. J. *Int. J. Quantum Chem.* **1998**, *33*, 87.
(15) Verslius, L.; Ziegler, T. *J. Chem. Phys.* **1988**, *88*, 322.
(16) Perdew, J. P.; Chevary, J. A.; Vosko, S. H.; Jackson, K. A.; Pederson, M. R.; Fiolhais, C. *Phys. Rev. B* **1992**, *46*, 6671.
(17) Clark, M.; Cramer, R. D. I.; van Opdenbosch, N. *J. Comput. Chem.* **1989**, *10*, 982.
(18) Woo. T. K.; Cavallo, L.; Ziegler, T. *Theor. Chim. Acta* **1998**, *100*, 307.
(19) Xu, Z.; Vanka, K.; Firman, T.; Michalak, A.; Zurek, E.; Zhu, C.; Ziegler, T. *Organometallics* **2002**, *21*, 2444.
(20) (a) Klamt, A.; Schuurmann, G. *J. Chem. Soc., Perkin Trans. 2* **1993**, 799. (b) Pye, C. C.; Ziegler, T. *Theor. Chem. Acta* **1999**, *101*, 396.

Table 3. Hydrogen Transfer Activation Energies (kcal/mol) for Different Counterions

	counterion		
cat.	$B(C_6F_5)_3Me^-$	$TMAMe^-$	TMA-$MAOMe^-$
$(Cp)(NC^tBu_2)TiMe^+$	21.9	26.5	28.2
$(Cp)(NP^tBu_3)TiMe^+$	23.3	30.5	28.9
$(Cp)(NC^tBu_2)ZrMe^+$	24.2	31.2	*a*
$(Cp)(NP^tBu_3)ZrMe^+$	26.5	32.9	*a*

[a] Not investigated.

1). Piers et al. have also compared the rates of decomposition of $[Cp(^tBu_2C{=}N)TiMe]^+[MeB(C_6F_5)_3]^-$ and $[Cp^*(^tBu_2C{=}N)TiMe]^+[MeB(C_6F_5)_3]^-$. The rate of decomposition of the C_5H_5-ligated complex is approximately 3 times faster than for the C_5Me_5-ligated systems. According to Piers et al., the Cp* system has a higher barrier of activation for hydrogen transfer due to the large electron-donating ability of the Cp* ligand. We partially agree with this assertion. However, we believe the observed difference in the kinetic stabilities of these systems is also due to steric factors. We find that the Cp* complex is kinetically more stable than the Cp system toward hydride transfer by 1.9 kcal/mol.

Stephan et al.[21] examined the electronic influence of different systems with similar steric properties on the catalytic activity. They observed a small difference in activity, but the trend suggests that electron-donating substituents favor a relatively higher activity. The same conclusion has been reached in a recent theoretical study.[18] Stephan et al. have also investigated the role of steric factors for electronically similar systems. The observed differences in activity show a remarkable dependence on steric factors. It was further underlined that steric rather than electronic factors are of prime importance for the generation of highly effective polymerization catalysts, again in agreement with theoretical predictions.[19] Stephan et al. have also mentioned the role of steric congestion in precluding deactivation pathways such as hydrogen transfer.

The calculations so far considered the very early stages of the polymerization when the growing chain is still represented by a relatively small methyl group. We have considered the hydrogen transfer of a later stage when the growing chain was represented by a *n*-pentyl group, to see if the increase in steric bulk would decrease the rate of hydrogen transfer. Replacing the growing chain with *n*-pentyl substituents does indeed increase the barrier by 5.8 kcal/mol for ketimide systems. It is thus clear that the rate of deactivation by hydrogen transfer will decrease as the chain starts to grow. We do not expect the barrier to increase substantially as the chain grows further.

Table 3 shows the effect of different counterions on the activation energies for hydrogen transfer. It is believed that the catalyst systems considered in this study perform at a significantly higher level when other types of counterions are employed. For comparison, the counterions considered are $TMAMe^-$ and TMA-$MAOMe^-$, where TMA = trimethylaluminum and MAO = methylaluminoxane, with $(AlOMe)_6$ taken as a representative model.[19] For the ketimide catalyst system, the hydrogen transfer barriers increase in the order $MeB(C_6F_5)_3^- <$ $TMAMe^- <$ TMA-$MAOMe^-$. The results suggest a considerable parallelism between ion-pair separation energies and hydrogen transfer barriers. The same order was observed for ion-pair separation energies in our previous work.[19] Thus, hydrogen transfer can be reduced if counterions with large ion-pair separation energies are employed. We have also compared the hydrogen transfer activation energies for the ketimide systems $[Cp(^tBu_2C{=}N)Ti(CH_3)_2]$ and $[Cp(^tBu_2C{=}N)TiMe]^+[MeB(C_6F_5)_3]^-$. The precatalyst (system without a counterion) is kinetically more stable than the catalyst by 9.0 kcal/mol toward hydride transfer.

Solvent effects were incorporated with full QM single-point solvent calculations on the optimized QM/MM geometries of the ion-pair and transition-state complexes. Cyclohexane ($\epsilon = 2.023$) was used as the solvent. As shown in Table 1, with R = ^{t}Bu, the gas-phase trend in activation energy for hydrogen transfer on changing the catalyst is valid. The trend in crossover temperature is also valid. However, there is a considerable shift of the crossover temperature because of an increase in activation energy for hydrogen transfer and a decrease in activation barrier for ethylene insertion. For example, the crossover temperatures for ketimide systems are 424, 513, and 571 K with $\Delta S^{\ddagger}_d = 0.0$, -2.7, and -8.5 cal/(mol K), respectively.

Optimized Transition-State Structures. The transition-state structures were optimized for all of the complexes for which we were able to calculate a barrier. During the transition-state search, the C−H bond from a methyl group in $[MeB(C_6F_5)_3]^-$ was broken and a C−H bond was partially formed in the growing chain. This is consistent with the large k_H/k_D isotopic effect observed for this reaction by Piers et al. Late transition states were predicted for most of the complexes. The ketimide and phosphinimide systems are discussed as representative examples. Figure 2 presents key optimized transition-state geometry parameters for these catalyst systems.

As shown in Figure 2, the Ti−C(methyl chain) distances are 2.285 and 2.311 Å for ketimide and phosphinimide, respectively. For the phosphinimide ligands, the Ti−N and N−P distances are 1.825 and 1.583 Å, respectively. These distances are in reasonable agreement with values reported for analogous equilibrium systems. Thus, a recent crystallographic investigation[21] of $(Cp)(NP^tBu_3)TiCl_2$ revealed Ti−N and N−P distances of 1.775 and 1.593 Å, respectively. The P−N−Ti bond angle calculated, 172.2°, is also in good agreement with the crystallographically determined value (176.6°) of the above system. The Ti−N distance (1.874 Å) for ketimide systems is longer than those seen in phosphinimide ligands, while the C−N−Ti angle (165.4°) is smaller than the corresponding P−N−Ti angle reported above. Piers and co-workers have reported a Ti−N distance of 1.830 Å and a C−N−Ti angle of 173.5° for ketimide systems. The X-ray crystal structure[22] of the related compound $(Cp)(^tBu^nBuC{=}N)TiCl_2$ showed a Ti−N distance of 1.872 Å and a C−N−Ti angle of 171.3°. Thus, our calculations and the X-ray crystallographically determined values predict longer Ti−N distances and

(21) Stephan, D. W.; Stewart, J. C.; Guerin, F.; Courtenay, S.; Kickhman, J.; Hollink, E.; Beddie, C.; Hoskin, A.; Graham, T.; Wei, P.; Spence, E. v. H.; Xu. Z.; Koch, L.; Gao, X.; Harrison, D. G. *Organometallics* **2003**, *22*, 1937.

(22) Lathman, I. A.; Leigh, G. J.; Huttner, G.; Jibril, I. *J. Chem. Soc., Dalton Trans.* **1986**, 377.

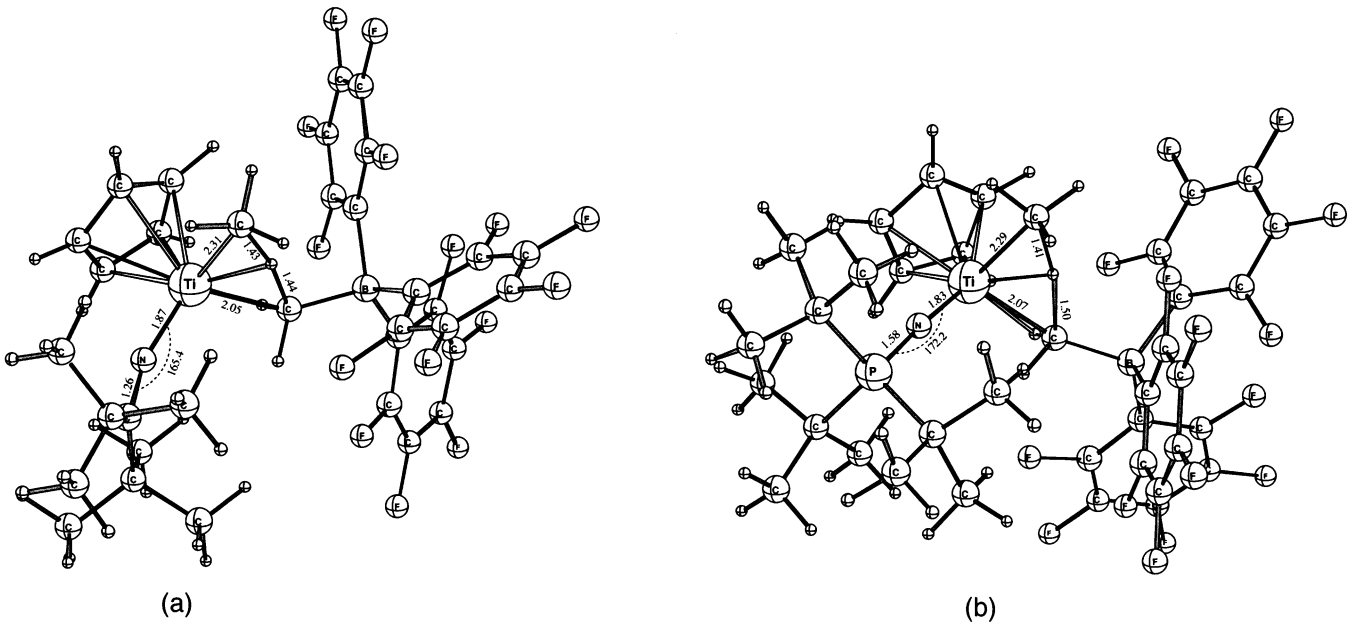

Figure 2. Optimized transition-state geometries (Å, deg) of ketimide (a) and phosphinimide (b).

smaller C−N−Ti angles relative to the corresponding Ti−N distances and P−N−Ti angles in phosphinimides. These differences presumably reflect the greater π-donor ability of the phosphinimide ligand relative to ketimides.

Effect of Entropy and Concentration on the Crossover Temperature. The thermal stability of olefin polymerization catalysts at high temperatures (around 100 °C) is a crucial prerequisite for industrial-scale applications. It is therefore important to compare rates of decomposition k_d and rates of propagation k_p. It is reasonable to consider the catalyst deactivates at a certain temperature T_x when the observed propagation rate k_p^{obsd} is equal to the rate of decomposition k_d. We shall refer to T_x as the crossover temperature. It should be noted that $k_p^{obsd} = k_p[M]$, where [M] is the concentration of monomer. Both rate constants under standard conditions can be expressed by using the Eyring equation, as shown below, where k_B is the Boltzmann constant and h is Planck's constant:

$$\ln\left(\frac{k_c}{T}\right) = \left(\frac{-\Delta H^{\ddagger}_c}{RT}\right) + \left(\frac{\Delta S^{\ddagger}_c}{R}\right) + \ln\left(\frac{K_B}{h}\right) \qquad (1)$$

$$c = d, p$$

Here $\Delta H^{\ddagger}_p$ and $\Delta H^{\ddagger}_d$ are the enthalpies of activation for the propagation and deactivation steps, respectively, whereas $\Delta S^{\ddagger}_p$ and $\Delta S^{\ddagger}_d$ are the corresponding entropies. We obtain by equating k_p^{obsd} and k_d and solving for T_x that

$$T_x = \frac{\Delta H^{\ddagger}_p - \Delta H^{\ddagger}_d}{\Delta S^{\ddagger}_p - \Delta S^{\ddagger}_d + R \ln [M]} \qquad (2)$$

The concentration term in eq 2 can be replaced with partial pressure, because we are dealing with gas-phase reactions. It should be noted that the propagation process in general must have a lower barrier than the decomposition process ($\Delta H^{\ddagger}_p < \Delta H^{\ddagger}_d$) for the catalyst to be active at any temperature. This is certainly the case with the hydrogen transfer process. Also, the propagation step is bimolecular, whereas the decomposition process under investigation is unimolecular; thus, $\Delta S^{\ddagger}_d > \Delta S^{\ddagger}_p$. Under these conditions one is ensured of obtaining a physically meaningful positive value for T_x. However, for bimolecular reactions one would either obtain a rather high T_x ($\Delta S^{\ddagger}_d \approx \Delta S^{\ddagger}_p$) or no crossover at all ($\Delta S^{\ddagger}_d < \Delta S^{\ddagger}_p$). Thus, bimolecular decomposition reactions are not as likely to be candidates for deactivation as unimolecular decomposition reactions.

It is difficult to obtain accurate experimental[23] or theoretical[24] estimates for the enthalpic and entropic parameters entering eq 2. We shall in the following adopt a common average value of $\Delta H^{\ddagger}_d = 12.0$ kcal/mol for the barrier to insertion of ethylene into the M−Me bond, in close agreement with the few available experimental[23] and theoretical[24] data. The barrier of decomposition ($\Delta H^{\ddagger}_d$) will, on the other hand, be taken from the calculated values in Tables 1 and 2.

Most problematic are the activation entropies. It is possible (but costly) to calculate theoretical $\Delta S^{\ddagger}$ values. Further, these values correspond to the gas phase and it is not easy to calculate the corresponding activation entropies in solution. We adopt for $\Delta S^{\ddagger}_p$ a value of −33 cal/(mol K) typical for a bimolecular insertion reaction.[23] The monomolecular decomposition reaction can be expected to have $\Delta S^{\ddagger}_d \approx 0.0$ cal/(mol K). For [Cp(^{t}Bu$_2$-C=N)TiMe]$^+$[MeB(C$_6$F$_5$)$_3$]$^-$, the observed[1d] $\Delta S^{\ddagger}_d$ value is −8.5 cal/(mol K), whereas we have obtained a theoretical gas-phase value of −2.7 cal/(mol K). We will make use of all three values for the entire set of titanium catalysts in order to gauge how a spread (uncertainty) of ∼10 cal/(mol K) influences the estimated T_x values.

A plot of $\ln(k_c/T)$ versus $1/T$ gives a straight line, as shown in Figure 3, where k_c is the rate constant for the propagation step or decomposition pathway. In all the simulations in Figure 3, the initial concentration was set to 1.0 M, corresponding to a pressure of 24.5 atm.

(23) Liu, Z.; Somsook, E.; White, C. B.; Rosaaen, K. A.; Landis, C. R. *J. Am. Chem. Soc.* **2001**, *123*, 11193.
(24) Vanka, K.; Xu, Z.; Ziegler, T. *Isr. J. Chem.* **2002**, *42*, 403.

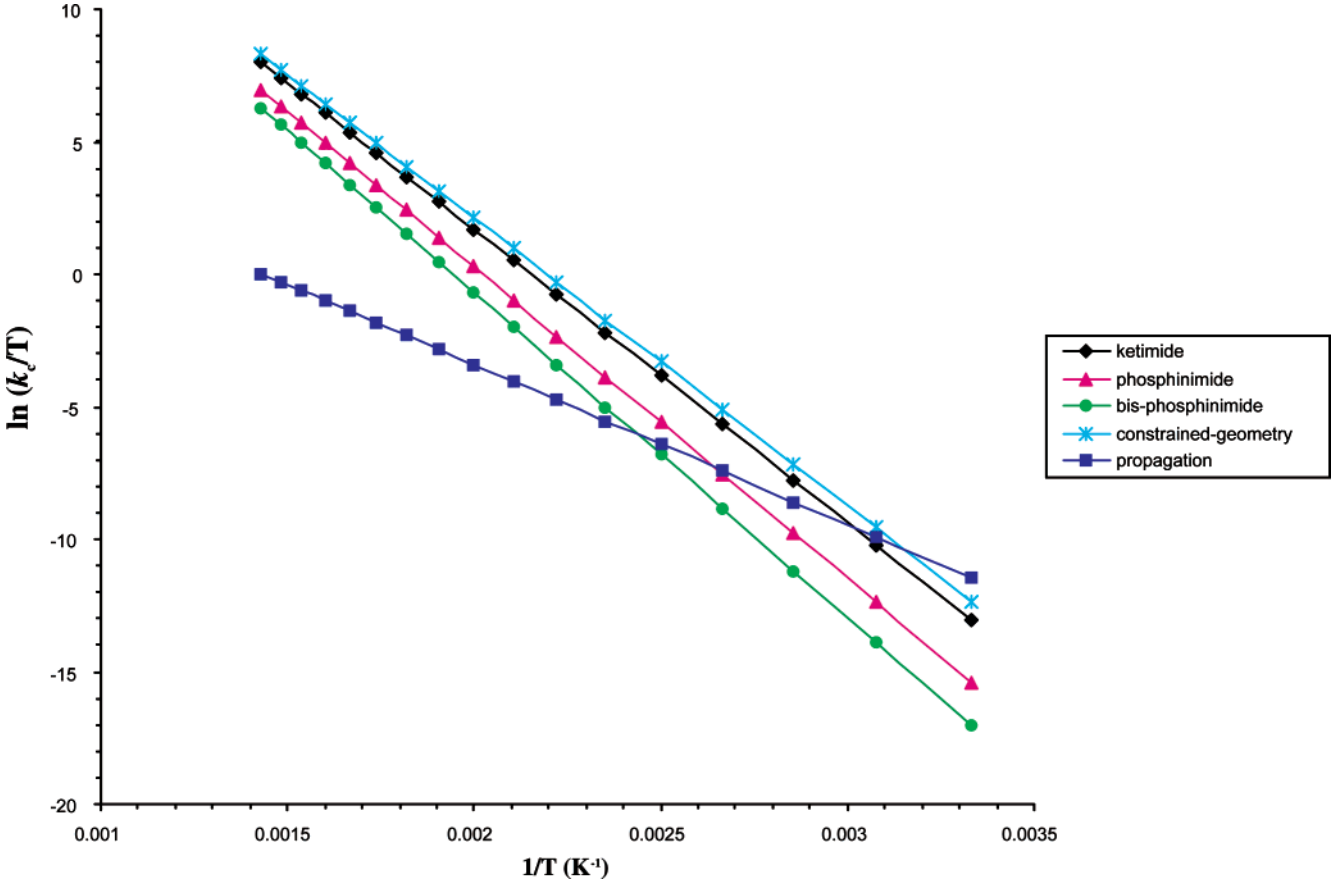

Figure 3. Plot of ln (k_c/T) vs. 1/T for different catalyst systems.

Table 4. Crossover Temperatures (K) at Three Different Activation Entropies[a]

cat.	$\Delta H^{\ddagger}_p$	$\Delta H^{\ddagger}_d$	$\Delta S^{\ddagger}_p$	$\Delta S^{\ddagger}_d$	T_x
(Cp)(NCR$_2$)TiMe$^+$	12.0	21.9	−33.0	0.0	300
	12.0	21.9	−33.0	−2.7	327
	12.0	21.9	−33.0	−8.5	404
(Cp)(NPR$_3$)TiMe$^+$	12.0	23.3	−33.0	0.0	342
	12.0	23.3	−33.0	−2.7	373
	12.0	23.3	−33.0	−8.5	461
(NPR$_3$)$_2$TiMe$^+$	12.0	24.3	−33.0	0.0	373
	12.0	24.3	−33.0	−2.7	406
	12.0	24.3	−33.0	−8.5	502
(Cp)(OSiR$_3$)TiMe$^+$	12.0	21.9	−33.0	0.0	300
	12.0	21.9	−33.0	−2.7	327
	12.0	21.9	−33.0	−8.5	404
(CpSiMe$_2$NR)TiMe$^+$	12.0	21.5	−33.0	0.0	288
	12.0	21.5	−33.0	−2.7	314
	12.0	21.5	−33.0	−8.5	388

[a] $\Delta S^{\ddagger}_p$ and $\Delta H^{\ddagger}_p$ values were taken from experimental data[22] and our previous work,[23] respectively. The counterion is B(C$_6$F$_5$)$_3$Me$^-$ in all cases.

Furthermore, $\Delta H^{\ddagger}_p = 12.0$ kcal/mol,[23,24] $\Delta S^{\ddagger}_p = -33.0$ cal/(mol K),[23] $\Delta S^{\ddagger}_d = -2.7$ cal/(mol K) (calculated value), and $\Delta H^{\ddagger}_d$ was taken from Table 1.

Tables 4 and 5 present the crossover temperature at different entropies of activation and concentrations. Here we shall illustrate the utility of simulated crossover temperatures (Table 4) for comparing the activity of the catalysts at higher temperatures (100−250 °C). For unimolecular reactions it may be argued that $\Delta S^{\ddagger}_d \approx 0$, since little reorientation of atoms is required to form the transition state in such processes. Thus, if $\Delta S^{\ddagger}_d = 0$, the crossover temperatures fall in the range 288−373 K, suggesting that none of the catalyst systems

Table 5. Crossover Temperatures (K) at Different Monomer Concentrations[a]

	monomer concn			
cat.	0.1 M	0.5 M	1.0 M	4.0 M
(Cp)(NCR$_2$)TiMe$^+$	285	314	328	361
(Cp)(NPR$_3$)TiMe$^+$	325	358	375	412
(NPR$_3$)$_2$TiMe$^+$	353	389	407	447
(Cp)(OSiR$_3$)TiMe$^+$	284	313	327	360
(CpSiMe$_2$NR)TiMe$^+$	273	301	314	346

[a] The counterion is B(C$_6$F$_5$)$_3$Me$^-$ in all cases.

considered in this study would survive above 100 °C. If $\Delta S^{\ddagger}_d = -2.7$ cal/(mol K) (calculated value), the crossover temperatures range from 314 to 406 K, reflecting that the bis(phosphinimide) and phosphinimide catalysts would survive above 100 °C. However, when $\Delta S^{\ddagger}_d = -8.5$ cal/(mol K) (experimental value for ketimide), we would get a different picture and the temperatures range between 388 and 502 K, suggesting the stability of all the catalyst systems at and above 100 °C. The bis(phosphinimide) and phosphinimide catalyst systems may still be active under harsher polymerization conditions close to 150 °C. However, it must be kept in mind that none of the catalyst systems would survive at 250 °C.

The temperature window can also be shifted if the concentration (partial pressure) of the monomer is increased, as shown in Table 5. If the concentration is increased from 1.0 to 4.0 M, the computed crossover temperatures range from 346 to 447 K, again indicating the stability of bis(phosphinimide) and phosphiminide catalysts at 100 °C. However, it should be borne in mind that the monomer concentration has to be increased to

Table 6. Total Bond Order around Ti and Hydrogen Transfer Activation Energies (kcal/mol) for Different Catalyst Systems

cat.	total bond order around Ti: ion pair	total bond order around Ti: TS	activation energy
(Cp)NPR_3TiMe-μ-MeB$(C_6F_5)_3$	4.36	4.42	23.3
(Cp)(NCR_2)TiMe-μ-MeB$(C_6F_5)_3$	4.18	4.21	21.9
$(CpSiMe_2NR)$TiMe-μ-MeB$(C_6F_5)_3$	4.24	4.31	21.5
$(NPR_3)_2$TiMe-μ-MeB$(C_6F_5)_3$	4.43	4.52	24.3
(Cp)$(OSiR_3)$TiMe-μ-MeB$(C_6F_5)_3$	4.31	4.40	21.9

such an extent that the observed rate of propagation k_p^{obsd} ($=k_p$[M]) is greater than the rate of decomposition.

Finally, it is noteworthy to consider the effect of the growing chain on the crossover temperature. Thus, replacing the methyl attached to the metal with an *n*-propyl or *n*-pentyl growing chain increases the activation barrier for the hydride transfer by 6.2 and 5.8 kcal/mol, respectively, for the ketimide systems. This increase corresponds to an increase in the crossover temperature by ~200 K, which raises T_x from 328 to 531 K. If we further take into account that the second and subsequent insertion barriers are somewhat lower (~9 kcal/mol[24]) than the first, one calculates a further increase of the crossover temperature from 531 to 630 K. Here the monomer concentration and the decomposition activation entropy were set to 1.0 M and −2.7 kcal/mol K, respectively. It is therefore clear that, if the catalyst can survive the first insertion, the systems discussed in Table 1 as well as their zirconium homologues would survive even at 250 °C.

Bond Order Analysis. A bond order analysis[25] was done to evaluate the total bonding around the titanium metal center in the ion-pair complexes as well as in the transition states. Table 6 summarizes the results obtained, along with the corresponding activation energies for the different systems.

From the results obtained, a clear correlation is observed between the activation barriers and the total bonding around the titanium metal center. The bis(phosphinimide) system has the highest activation barrier, as well as the highest bond order around the titanium metal center, in both the ion-pair complexes and the transition states. The phosphinimide system is second highest in terms of both the activation energies and the bonding around the titanium. A reasonable correlation exists for the three systems, the ketimide, the siloxy, and the constrained-geometry catalyst, between the bonding around the metal center and the corresponding activation barriers**.** However, there is a switch between the constrained-geometry catalyst and ketimide systems.

The explanation for this correlation lies in the ion-pair separation energies of the catalyst systems. As shown in our previous work,[19] the ion-pair separation energies decrease in the order CGC > ketimide > siloxy > phosphinimide > bis(phosphinimide).

Therefore, the two NPR_3 groups in bis(phosphinimide) provide the greatest electron density to the metal center, as evidenced by the lowest ion-pair separation energy and the highest bond order around Ti. The constrained-geometry catalyst and ketimide provide the least electron density to the metal center. This, in turn, implies that the bonding between the titanium and the alkyl chain is strongest for the bis(phosphinimide) and weakest for the ketimide and CGC systems. Now, for the hydrogen transfer reaction to take place, the carbon in the μ-methyl bridge has to lose a hydrogen to the accepting α-carbon in the alkyl chain (see Scheme 1). This is most likely for the CGC and the ketimide systems, because the bonding between the α-carbon in the alkyl chain and the titanium is weakest here, as explained above. Hence, the corresponding lower activation barriers observed for the two systems. Moreover, since the bonding between the α-carbon in the alkyl chain and the titanium is the strongest in the bis(phosphinimide) system (as explained above), the activation barrier is the highest for this system.

Conclusions

Hydrogen transfer from $[MeB(C_6F_5)_3]^-$ to the growing chain of L_2MR^+ (M = Ti, Zr) is a possible deactivation pathway for olefin polymerization catalysts of the type $L_2MR^+[MeB(C_6F_5)_3]^-$ in the initial stage of the polymerization process when R = CH_3. Electron-donating bulky ancillary ligands attached to the cationic metal center, M, play a major role in increasing the transfer barrier. However, with methyl as the growing chain, all the titanium-based catalysts examined here are predicted to decompose above 100 °C. The rate of hydrogen transfer will be reduced as the growing chain increases in size, with the result that the titanium-based catalysts might sustain temperatures as high as 250 °C before decomposition. The titanium systems are more likely to decompose than the zirconium catalysts. This reflects the fact that the M−C bond is stronger for M = Zr than M = Ti.

The entropy of activation and the concentration of the monomer can strongly modulate the decomposition temperature. For example, if $\Delta S^{\ddagger}_d = 0$, none of the catalyst systems under investigation in this study would survive above 100 °C with R = CH_3. If we consider the computed activation entropy ($\Delta S^{\ddagger}_d = -2.7$ cal/(mol K)), the bis(phosphinimide) and phosphinimide systems would be active above 100 °C with R = CH_3. However, if we use the experimental activation entropy (−8.5 cal/(mol K)), all the catalyst systems would survive at 100 °C. The bis(phosphinimide) and phosphinimide catalysts may still be active under harsh polymerization conditions such as 150 °C with R = CH_3. Furthermore, deactivation could also be eliminated if the concentration of the monomer is increased to such an extent that k_p[M] > k_d.

Acknowledgment. This work was supported by the Natural Science and Engineering Research Council of Canada (NSERC) and by NOVA Research and Technology Corp. (NRTC). We thank Dr. Sven Tobisch for the frequency calculations.

Supporting Information Available: Cartesian coordinates (Å) for all optimized (QM/MM) ion-pair and transition-state (TS) geometries. This material is available free of charge via the Internet at http://pubs.acs.org.

OM034232T

(25) Michalak, A.; DeKock, R. L.; Ziegler, T., Manuscript in preparation. The bond order method employed in this work is a modification of that published by Nalewajski and co-workers. (a) Nalewajski, R. F.; Mrozek, J. *Int. J. Quantum Chem.* **1994**, *51*, 187. (b) Nalewajski, R. F.; Mrozek, J.; Michalak, A. *Int. J. Quantum Chem.* **1997**, *61*, 589.